Acta Crystallographica Section B
Structural Science
ISSN 0108-7681

Detailed example of the identification and crystallographic analysis of a pseudo-merohedrally twinned crystal

Ilia Guzei,[a]* Regine Herbst-Irmer,[b] Apollinaire Munyaneza[c] and James Darkwa[d]

[a]Department of Chemistry, University of Wisconsin–Madison, 1101 University Av., Madison, WI 53558, USA, [b]Department of Structural Chemistry, University of Göttingen, Tammannstrasse 4, D-37077 Göttingen, Germany, [c]Department of Chemistry, University of Botswana, Private Bag UB00704, Gaborone, Botswana, and [d]Department of Chemistry, University of Johannesburg, Auckland Park Kingsway Campus, PO Box 524, Johannesburg, South Africa

Correspondence e-mail: iguzei@chem.wisc.edu

Received 30 November 2011
Accepted 21 January 2012

A detailed description of the procedures utilized in the non-routine X-ray single-crystal structural determination and refinement of a pseudo-merohedrally twinned crystal of an Fe/Ni organometallic complex is presented. It illustrates to the practitioners of crystallography how to properly handle such cases and describes the logic and concrete steps necessary to account for the twinning, pseudo-symmetry and atomic positional disorder.

1. Introduction

Only 50 years ago X-ray structural determination was regarded as a difficult, time-consuming process which could only be carried out by highly trained crystallographers; current instrumentation and software have made this technique available to the chemists as a routine analytical technique. Today high-quality crystal structures, especially those of small molecules, are obtained by synthetic organic and inorganic chemists within days or even hours. Single-crystal X-ray analysis has developed into the most powerful method for obtaining the atomic arrangement in the solid state. Nowadays the rate-determining step for X-ray analysis generally involves the preparation of suitable single crystals.

The use of modern X-ray software has normally allowed the facile detection of twinned crystals. Nonetheless, correct handling of the different kinds of crystal twinning is still a major issue because crystallographic software does not automatically detect the correct twin laws, especially when the usual structural solution and refinement methods do not give rise to unambiguous results, as primarily shown by non-convergence of the discrepancy indices (such as wR_2) between observed and calculated F^2 data.

According to the *International Tables for Crystallography* 'a twin consists of two or more single crystals of the same species but in different orientations, its *twin components*' (Wilson, 1995). In merohedral twins the twin law is a symmetry operator of the crystal system, but not of the point group of the crystal (possible twin operations for twins by merohedry are listed in *International Tables for Crystallography*). In non-merohedral twins the twin operation belongs neither to the crystal class of the structure nor to the metric symmetry of the unit cell. In pseudo-merohedral twins the twin law belongs to a higher crystal system than the structure (Herbst-Irmer, 2006). This may happen if the metric symmetry is higher than the symmetry of the structure, or when it mimics a higher-symmetry crystal class. Herein we will concentrate on pseudo-merohedral twinning.

During the design of the Basílica i Temple Expiatori de la Sagrada Família in Barcelona, architect Antoni Gaudí found

inspiration, among other things, in twinned crystals. Whereas twinned crystals can be visually stunning, practical aspects of their structural characterization are frequently less fascinating. Pseudo-merohedrally twinned structures are reported on a regular basis. A search of the International Union of Crystallography journals for the key words 'pseudo-merohedral twin' returned only 65 hits for years 2006–2011, of which 11 papers were published in *Acta Cryst.* (Sections B and C). Recently, an example of pseudo-merohedral twinning in the structure of nonactin (Guzei *et al.*, 2009) and a case of treatment of a non-merohedral twinning as pseudo-merohedral in the structure of cyclopentadecanone (Noe *et al.*, 2008) were published. Whereas a number of crystallographic publcations provide background information on twinning (Herbst-Irmer & Sheldrick, 1998, 2002; Herbst-Irmer, 2006; Lebedev *et al.*, 2006; Parsons, 2003; Wilson, 1995; Zwart *et al.*, 2008), the majority of these publications report only the results of crystallographic studies with minimal technical details of nuances of twin handling. Herbst-Irmer & Sheldrick (1998, 2002; Herbst-Irmer, 2006) have described examples of twin refinement. Moreover, their crystallographic publications list 13 warning signs of twinning (ST), of which the following are relevant for the study presented herein:

(ST1) The metric symmetry is higher than the Laue symmetry.

(ST2) The $R_{\rm sym} = \sum |F_{\rm o}^2 - \langle F_{\rm o}^2 \rangle| / \sum F_{\rm o}^2$ value for the higher-symmetry Laue group is only slightly higher than that for the lower-symmetry Laue group.

(ST3) The mean value for $|E^2 - 1|$ is much lower than the expected mean value of 0.736 for a non-centrosymmetric space group.

(ST4) Indicated systematic absences are inconsistent with those for any known space group.

(ST5) $K = \langle F_{\rm o}^2 \rangle / \langle F_{\rm c}^2 \rangle$ is systematically high for reflections with low intensity.

(ST6) For all the 'most disagreeable' reflections, generally $F_{\rm o} \gg F_{\rm c}$.

This paper reports the detailed crystal structure and refinement of the Fe/Ni complex {bromo[di-(3-ferrocenyl-5-ethylcarboxylate-pyrazolyl-1-ylmethyl)pyridine]nickel(II)} tetrabromoferrate(III) (1) (see Scheme 1 and Fig. 1), which posed a particularly challenging problem. The latter stemmed from the pseudo-symmetry of the structure along with the absence of a detailed published X-ray tutorial that may help one tackle a case of pseudo-merohedral twinning. A detailed discussion of a related case is presented by Guevarra *et al.* (2005). In the Donnay nomenclature, this is an example of twinning by twin-lattice symmetry, TLS, class II (Donnay & Donnay, 1974). The high-quality data ultimately allowed us to identify and resolve the twinning/symmetry problem and to correctly refine the structure. Although this structure was not particularly difficult to solve, it proved to be very difficult to refine due to the ambiguity of the correct Bravais lattice type and space group caused by near-perfect pseudo-merohedral twinning combined with pseudo-symmetry. To demonstrate how such a refinement could be handled the structural determination of (1) will be scrupulously described.

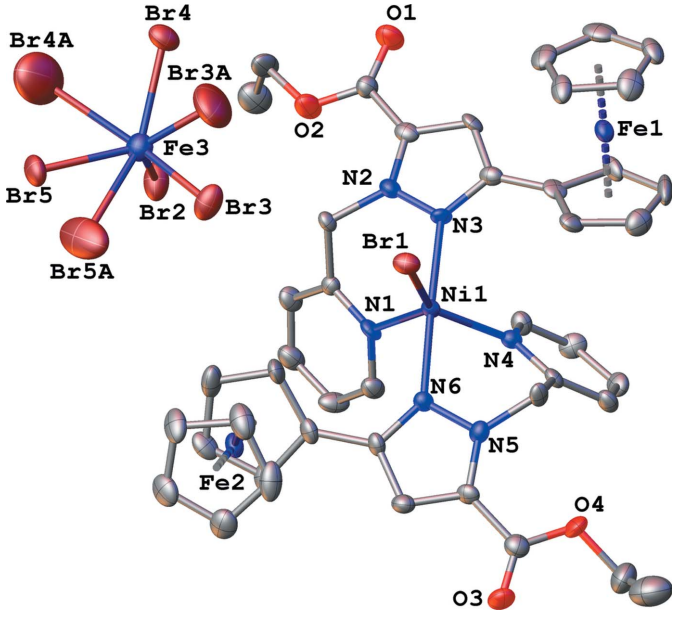

Figure 1
A molecular drawing of (1) showing the atomic arrangement of the trigonal bipyramidally coordinated Ni{N_4Br} and crystal-disordered $[FeBr_4]^-$ monocation with 50% probability ellipsoids (Dolomanov *et al.*, 2009). All H atoms are omitted. Atoms Br3–5 of the tetrahedral anion $[FeBr_4]^-$ anion are disordered over two positions; the major component has a site occupancy of 85.5 (2)%.

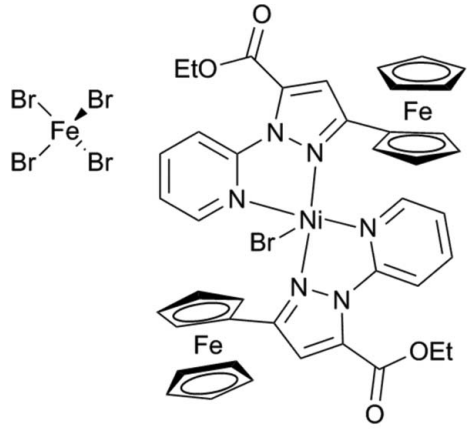

Scheme 1

2. Experimental

2.1. X-ray crystallography

2.1.1. Instrumentation. X-ray data acquisition was conducted on a Bruker AXS APEX2 diffractometer equipped with a sealed-tube Cu $K\alpha$ radiation source and an Oxford Cryostream 700 cooling device. The Oxford Cryostream 700 was carefully calibrated in the range 100–400 K with a Si diode model DT-421-HR-4 L (DT-421 miniature silicon diode) and a temperature monitor model 211, both from Lakeshore Cryotronics, Inc.

Table 1
Experimental details.

Crystal data	
Chemical formula	$C_{44}H_{42}Br_5Fe_3N_6NiO_4$
M_r	1344.65
Crystal system, space group	Monoclinic, *Cc*
Temperature (K)	100
a, *b*, *c* (Å)	15.2181 (3), 22.0080 (3), 16.0005 (3)
β (°)	118.393 (2)
V (Å^3)	4714.25 (14)
Z	4
Radiation type	Cu $K\alpha$
μ (mm^{-1})	13.07
Crystal size (mm)	0.19 × 0.11 × 0.09
Data collection	
Diffractometer	Bruker SMART APEX2 area detector
Absorption correction	Analytical *SADABS* (Bruker-AXS, 2007)
T_{min}, T_{max}	0.186, 0.376
No. of measured, independent and observed [$I > 2\sigma(I)$] reflections	35 920, 8033, 7903
R_{int}	0.031
Refinement	
$R[F^2 > 2\sigma(F^2)]$, $wR(F^2)$, S	0.032, 0.078, 1.05
No. of reflections	8033
Bijvoet pair coverage (%)	86
No. of parameters	599
No. of restraints	4
H-atom treatment	H-atom parameters constrained
$\Delta\rho_{max}$, $\Delta\rho_{min}$ (e Å^{-3})	0.70, −0.66
Absolute structure	Flack (1983)
Flack parameter	−0.008 (4)

Computer programs: *APEX2* (Bruker, 2007), *SAINT* (Bruker, 2011*b*), *SHELXTL* (Sheldrick, 2008*a*).

2.1.2. X-ray data collection. The relevant crystallographic information for (1) is tabulated in Table 1. A full-sphere dataset to a resolution of 0.82 Å was obtained in routine fashion with Cu $K\alpha$ radiation on a yellow crystal with approximate dimensions 0.19 × 0.11 × 0.09 mm^3 at 100 K. The acquired scans were integrated using *SAINT* (Bruker, 2011*b*) and the highly redundant final dataset was corrected for Lorentz and polarization effects. The absorption correction was based on the fitting of a function to the face-indexed transmission surface, as sampled by multiple equivalent measurements using *SADABS* (Bruker AXS Inc., 2011*a*). For details of the structural solution and refinement, see §§3.3 and 3.5.

2.1.3. Synthesis. Preparation of {bromo[di-(3-ferrocenyl-5-ethylcarboxylate-pyrazolyl-1-ylmethyl)pyridine]nickel(II)} tetrabromoferrate(III). A mixture of (3-ferrocenyl-5-ethyl-carboxylate pyrazolyl-1-ylmethyl)pyridine (0.050 g, 0.146 mmol) and $NiBr_2$ (0.016 g, 0.073 mmol) in ethanol (10 ml), prepared by the literature procedure (Guzei *et al.*, 2012), was stirred at room temperature for 18 h. After 15 min the color of the solution started changing progressively from light yellow to intense yellow. The solution was evaporated to dryness, and the residue re-crystallized by a slow evaporation of a dichloromethane–toluene (3:1) solution of the crude product at room temperature. Crystals of the product were isolated by filtration and dried. Yield: 0.045 g (83%). $C_{44}H_{42}N_6Br_5O_4Fe_3Ni$: calc: C 39.30, H 3.15, N 6.25; found: C 39.65, H 3.10, N 6.15%.

3. X-ray crystallography and twinning

3.1. Unit-cell and data collection

The initial unit-cell determination was straightforward. The reflections of the intensity-weighted reciprocal lattice showed no sign of splitting and could be successfully indexed with a single orientation matrix with the automated *APEX2* indexing routines and program *CELL_NOW* (Sheldrick, 2008*b*). The metric parameters were consistent with an *F*-centered orthorhombic lattice. A full sphere of data was collected and after numerical correction for absorption with *SADABS* the data were merged to an acceptable R_{sym} value of 0.060 (Table 2, option A).

3.2. Space-group determination

The program *XPREP* (Sheldrick, 2006) was used for data examination. In the following discussion options A–F refer to Table 2. The default values of the program menu choices led to the lone option A of an *F*-centered orthorhombic unit cell. The choice of this pseudo-orthorhombic face-centered lattice subsequently indicated the absence of a plausible known space group consistent with the observed systematic absences (recall ST4). The reflection conditions clearly manifested the presence of a single diamond glide perpendicular to the *b* axis, but at least one additional *d*-glide plane perpendicular to another axis required by symmetry was decidedly absent. Nonetheless, the likeliest known candidate space group *Fdd*2 was chosen. An alternative space-group determination with the program *PLATON* (Spek, 2009) also suggested *Fdd*2. Indeed, the structure *could* be solved in this space group (the order of space group, Z = 8; the number of molecules in the

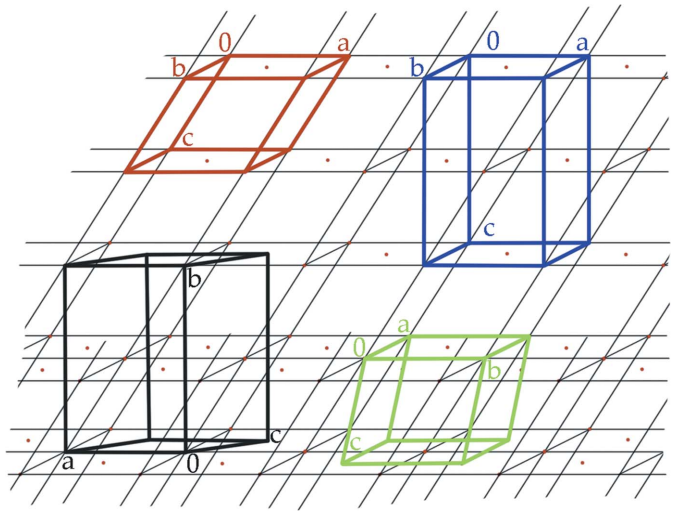

Figure 2
Clockwise from top left: red – C-centered monoclinic cell (option F, Table 2); blue – pseudo-orthorhombic F-centered cell (option A); green – monoclinic C-centered cell (option B); black monoclinic C-centered cell (option D). The red dots represent lattice points.

Table 2
Possible unit-cell choices for (1).

This table was produced with program *XPREP* after adjustment of the 'tolerance' with options *T*, and *T* again, and a setting of 0.00°. The 'matrix' lines indicate the transformations from a triclinic cell chosen for integration to ensure that no symmetry was missed.

Identical indices and Friedel opposites combined before calculating R(sym)
Option A: FOM = 0.026° ORTHORHOMBIC F-lattice R(sym) = 0.060 [6049] Cell: 15.218 22.008 28.151 89.98 90.00 89.99 Volume: 9428.45 Matrix: −1.0000 −1.0000 0.0000 −1.0000 1.0000 0.0000 −1.0000 −1.0000 −2.0000
Option B: FOM = 0.014° MONOCLINIC C-lattice R(sym) = 0.052 [3988] Cell: 22.008 15.218 17.863 89.99 128.00 90.01 Volume: 4714.23 Matrix: −1.0000 1.0000 0.0000 1.0000 1.0000 0.0000 0.0000 −1.0000 −1.0000
Option C: FOM = 0.014° MONOCLINIC I-lattice R(sym) = 0.052 [3988] Cell: 17.863 15.218 17.870 90.01 103.97 90.01 Volume: 4714.23 Matrix: 0.0000 1.0000 1.0000 1.0000 1.0000 0.0000 −1.0000 0.0000 −1.0000
Option D: FOM = 0.022° MONOCLINIC C-lattice R(sym) = 0.059 [3941] Cell: 15.218 28.151 13.377 89.98 124.65 90.00 Volume: 4714.23 Matrix: 1.0000 1.0000 0.0000 1.0000 1.0000 2.0000 0.0000 −1.0000 0.0000
Option E: FOM = 0.022° MONOCLINIC I-lattice R(sym) = 0.059 [3941] Cell: 13.377 13.380 89.98 110.67 90.02 Volume: 4714.23 Matrix: 0.0000 1.0000 0.0000 1.0000 1.0000 2.0000 1.0000 0.0000 0.0000
Option F: FOM = 0.026° MONOCLINIC C-lattice R(sym) = 0.036 [3905] Cell: 15.218 22.008 16.000 89.99 118.39 89.99 Volume: 4714.23 Matrix: −1.0000 −1.0000 0.0000 −1.0000 1.0000 0.0000 0.0000 0.0000 −1.0000
Option G: FOM = 0.000° TRICLINIC P-lattice R(sym) = 0.000 [0] Cell: 13.377 13.380 16.000 105.68 105.70 110.67 Volume: 2357.11 Matrix: 0.0000 −1.0000 0.0000 −1.0000 0.0000 0.0000 0.0000 0.0000 −1.0000

asymmetric unit, $Z' = 0.5$) with the cation and anion each occupying a crystallographic twofold axis. The overall molecular connectivity could be established with the exception of the methyl C atoms, but the refinement was computationally unstable and did not converge. It was also noticed that the mean value of the $|E^2 - 1|$ (0.608) was significantly lower than the value of 0.736 expected for a non-centrosymmetric space group (recall ST3). These indicators along with a glaring ST6 warning ($F_o \gg F_c$ for the most poorly fitting reflections) were diagnostic signs of pseudo-merohedral twinning (Herbst-Irmer & Sheldrick, 1998). The symmetry was then lowered from orthorhombic to monoclinic in order to determine the correct space group.

XPREP was restarted and the threshold value (in degrees) for the termination of cell searches was changed from the default value of 0.05° to zero (see the supplementary material[1] for details and the *XPREP* listing file). All monoclinic options looked reasonable and were sequentially examined.

Table 2 shows an analysis of possible symmetry-lowering routes in terms of the crystal system and merging statistics. There were two pairs of equivalent monoclinic unit cells in the table, options B/C and D/E, with figures of merit and merging R_{sym} slightly lower than that for the pseudo-orthorhombic *F*-centered cell (option A) and a third monoclinic option F with even better values. Fig. 2 depicts the cell choices. For illustrative purposes we will describe all three possibilities although an experienced crystallographer would probably start with the last option F (the reasons are outlined below). Although B and D show the standard *C*-centered lattice setting, we chose C and E with a non-standard *I*-centered lattice, because with these unit cells the twin law is easier to derive: the *a* and *c* axes have very similar lengths, and twinning could be accounted for by the introduction of a transformation matrix swapping the *a* and *c* axes and inverting the *b* axis.

For option C there were no clear systematic absences for a *c*-glide plane (previously seen in the form of a *d*-glide perpendicular to the *a* axis in the orthorhombic setting). Therefore, the structural solution was attempted in space group *I*2, but failed. The structure could be solved in space group *Ic*; however, as in the case of *Fdd*2, the overall geometry of (1) could be established except for the methyl C atoms. This *I*-centered refinement with a twin law involving the interchanging of the *a* and *c* axes, matrix = (0 0 1 / 0 $\overline{1}$ 0 / 1 0 0), unexpectedly produced a refinement with improved numerical indicators, such as substantially lower *R* factors, but the overall geometry of (1) inexplicably fell apart beyond repair.

The resulting situation for the *I*-centered option E was similar. The crystal structure could be solved in the space group *I*2 ($Z = 4$, $Z' = 1$) with two symmetry-independent half-anions and two half-cations residing on crystallographic twofold axes. Again there were refinement problems and the introduction of the twin law (0 0 1 / 0 $\overline{1}$ 0 / 1 0 0) improved the *R* values but not the model.

Option F belongs to a *C*-centered monoclinic unit cell with a clearly lower R_{sym} value, which is the lowest among the non-triclinic space groups (ST1, ST2). This difference from that of the pseudo-orthorhombic R_{sym} might be explained by the much greater number of (would be) equivalent reflections in the orthorhombic case, but the magnitudes of the R_{sym} values should be similar for all three monoclinic possibilities in the case of a true orthorhombic structure. The *C*-centered monoclinic space group (option F) was ultimately demonstrated to be correct.

3.3. Structural solution and twin refinement for option F

In the *C*-centered monoclinic setting systematic absences for a *c*-glide were found. The crystal structure could be successfully solved in the space group *Cc* by the application of direct methods (Sheldrick, 2008*a*). All non-H atoms were located in the difference-Fourier map (it should be noted that difference-Fourier maps can be troublesome in the case of twinning), and the disorder in the $[FeBr_4]^-$ anion was modeled over the course of several least-squares refinement cycles. Still, the C atoms of the methyl groups could not be located. In addition, the *R*1 factor stabilized at ~ 0.17, and many atomic displacement ellipsoids were exceedingly prolate/oblate.

[1] Supplementary data for this paper are available from the IUCr electronic archives (Reference: PS5014). Services for accessing these data are described at the back of the journal.

The structure exhibited classic signs of twinning (ST3-6). The E statistic $|E^2 - 1| = 0.619$ was much lower than that of 0.736 expected for a non-centrosymmetric structure. The R_{sym} value for the higher-symmetry pseudo-orthorhombic Laue group was only slightly higher than for the true space group, and the ratio $K = F_o^2/F_c^2$ was systematically high for low-intensity reflections. For almost all the most poorly fitting reflections the observed F_o structure factors were much greater than the F_c ones. The program *PLATON* was then employed to analyze the data, and pseudo-merohedral twinning was detected (see the supplementary material for a *PLATON* listing file). The suggested transformation matrix (1 0 0 / 0 $\bar{1}$ 0 / $\bar{1}$ 0 $\bar{1}$) corresponds to a 180° rotation about the crystallographic *a* axis.

When refining a twinned crystal structure it is necessary to input the twin law into the refinement program being used, and to specify a parameter which represents the twin component ratio. In *SHELXL* this is accomplished by adding the following two lines to the instruction file:

TWIN 1 0 0 0 −1 0 −1 0 −1 2

BASF 0.4

The TWIN line provides the transformation matrix and the number of the twin domains; the batch scale factor BASF provides an initial value for the minor domain contribution. There is a number of statistical tests that can help estimate the twin component ratio. Some fail if the twinning is perfect (the twin component ratio is 1:1); those that work may produce an inaccurate estimate; but in practice starting with an educated guess is just faster. The refinement showed a marked improvement (the R factor dropped to $\sim$ 0.07) and indicated a 46% contribution from a second twin component.

Option F would probably have been the first choice for the following reasons:

(i) There was no plausible known space group for an orthorhombic *F*-centered cell with systematic absences for one diamond glide, and the value for $|E^2 - 1|$ value was lower than expected (ST1, ST2). Hence, the structure is instead probably monoclinic and twinned.

(ii) Of the three monoclinic possibilities option F showed the lowest R_{sym} value.

(iii) Only in option F were there clear systematic absences corresponding to a known space group (*Cc*).

In addition, it is advisable to take the twinning into account from the beginning of the refinement, because this may make Fourier maps simpler to interpret. When a twin law is used from the beginning the warning signs ST5 and ST6 cannot be seen, but a successful refinement of a twinned crystal structure is the best proof of twinning.

Pseudo-merohedral twinning in a non-centrosymmetric space group requires additional caution, because the determination of the absolute structure is also necessary. Indeed, here the program *XL* produced a warning regarding the (in)correctness of the absolute structure, and the shapes of some atomic displacement ellipsoids were still excessively oblate and prolate. In the case of a twinned non-centrosymmetric structure the absolute structure of both twin domains must be checked, because additional racemic twinning may occur.

The means by which the addition twin operators are incorporated into the refinement model is program-specific. In *SHELXL* it can be accomplished with the modified TWIN and BASF commands:

TWIN 1 0 0 0 −1 0 −1 0 −1 −4

BASF 0.46 0.2 0.2

Note the presence of the '−4' on the TWIN line to multiplicatively refine the inversion operation for each twin domain, because four twin components may be present. The three parameters of the BASF line correspond to three out of four domains; a fourth is not needed as the sum of the component scales must be unity.

The component scale factors refined to:

BASF 0.464 0.546 −0.004

The scale factors (*K*-numbers below) describe the four twin domains in Table 3.

These values indicate that there are only two twin domains (*K*2 and *K*3). Since the main domain *K*1 is not present but domain *K*3 is, the current absolute structure is wrong (see matrix for *K*3). This requires us to invert the structure to make domain *K*3 the major twin component.

The atomic coordinates are easily inverted (with *SHELXL* command MOVE 1 1 1 −1) to reference component *K*3. It follows that the second twin component [*K*2 = 0.464 (4)] would also have to be inverted with the transformation matrix changed from (1 0 0 / 0 $\bar{1}$ 0 / $\bar{1}$ 0 $\bar{1}$) to ($\bar{1}$ 0 0 / 0 1 0 / 1 0 1). Note that the latter matrix corresponds to a mirror reflection in the b^*c^* plane. An alternative and preferred description of the twin matrix is a symmetry-related matrix corresponding to a twofold rotation axis parallel to the c^* axis: ($\bar{1}$ 0 0 / 0 $\bar{1}$ 0 / 1 0 1) (Fig. 3). Whereas the two descriptions are mathematically equivalent, we prefer the latter because a rotation can be related to the C_2 pseudo-symmetry in the structure of (1) (see

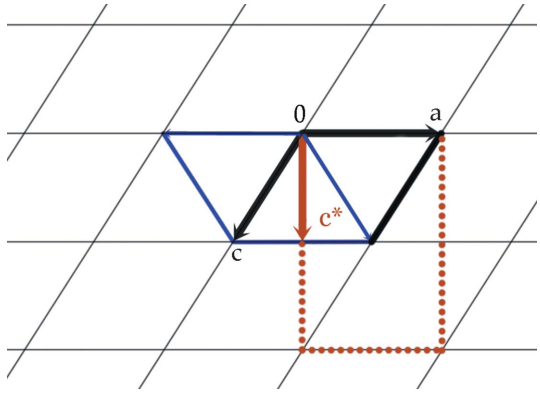

Figure 3
Crystal twinning in the structure of (1). Black – monoclinic *C*-centered unit cell (option F); blue – the unit cell related to it by 180° rotation about c^*; the red dotted line corresponds to the apparent orthorhombic unit cell (option A). The monoclinic *b* axis is perpendicular to the *ac* plane. Due to the nearly exact orthorhombic metric symmetry the overlap of the two reciprocal lattices is exact within experimental error.

Table 3
The scale factors (*K* numbers) describing the four twin domains.

Component	Relationship	Contribution
*K*1 (= 1 − *K*2 − *K* − *K*4)	$\begin{pmatrix} 1 & 0 & 0 \\ 0 & 1 & 0 \\ 0 & 0 & 1 \end{pmatrix}$	0.000 (4)
*K*2	$\begin{pmatrix} 1 & 0 & 0 \\ 0 & \bar{1} & 0 \\ \bar{1} & 0 & \bar{1} \end{pmatrix}$	0.464 (4)
*K*3	$\begin{pmatrix} \bar{1} & 0 & 0 \\ 0 & \bar{1} & 0 \\ 0 & 0 & \bar{1} \end{pmatrix}$	0.546 (4)
*K*4	$\begin{pmatrix} \bar{1} & 0 & 0 \\ 0 & 1 & 0 \\ 1 & 0 & 1 \end{pmatrix}$	0.004 (4)

below) and because programs such as *XPREP* and *PLATON* only use rotations. The number of the batch scale parameters could be reduced to one because there is only one configuration of each component (note that component *K*4 was absent). The final refinement with the following commands in the instruction file:

MOVE 1 1 1 −1
TWIN −1 0 0 0 −1 0 1 0 1 2
BASF 0.46

proceeded smoothly to yield an *R* factor of < 0.04 together with a very reasonable geometry of (1). Both methyl C atoms could now be located and satisfactorily refined.

To complete the refinement, the frame data were reintegrated in the correct monoclinic *C*-centered unit cell and numerically corrected for absorption. We also collected data on a different crystal of this compound with Mo *Kα* radiation and obtained comparable but worse results, presumably due to the use of an older SMART-1000 detector.

This is an elegant example of a pseudo-merohedrally twinned structure in which the absolute structure of both domains could be reliably established. Both crystals have the same structure, only with a different spatial orientation.

3.4. An alternative derivation of the twin law

The Ni^{II} cation of (1) approaches a non-crystallographic twofold rotational symmetry. The non-H atoms of this complex can be superimposed on their 180° rotated equivalents with a r.m.s of 0.24 Å, provided that the Me C atoms are excluded. When a non-crystallographic symmetry axis is close to a crystallographic axis, pseudo-symmetry may arise. The rotational pseudo-symmetry axis in such a case may become a twin axis. Compound (1) precisely exhibits this behavior. Moreover, in this case the twinning is near-perfect with a 0.54:0.46 component ratio, which made the detection of a twinned structure more difficult.

In the structure of (1) solved under the known orthorhombic space group *Fdd*2 the Ni^{II} cation resides on a twofold symmetry axis. We now know that the correct space group is *Cc*, a maximal isomorphous subgroup of *Fdd*2 (recall that the systematic absences were consistent with the not-allowed *F*1*d*1 but not the allowed *Fdd*2). In the correct space group *Cc* the pseudo-symmetry axis [102] that coincides with the *c** vector forms a 2.0° angle with the Ni1–Br1 vector of the cation and a 4.2° angle with the Fe3–Br2 vector of the anion. To derive the twin law for space group *Cc* we must multiply three matrices. The first transforms *oF* → *mC*, the second corresponds to the twofold rotation about the *c* axis in *Fdd*2, and the third converts *mC* → *oF*, which is the inverse of the first matrix. The product is the same matrix as that we used above which is equivalent to the one proposed by *PLATON*:

$$\begin{pmatrix} \bar{1} & 0 & 0 \\ 0 & \bar{1} & 0 \\ \frac{1}{2} & 0 & \frac{1}{2} \end{pmatrix} \times \begin{pmatrix} \bar{1} & 0 & 0 \\ 0 & \bar{1} & 0 \\ 0 & 0 & 1 \end{pmatrix} \times \begin{pmatrix} \bar{1} & 0 & 0 \\ 0 & \bar{1} & 0 \\ 1 & 0 & 2 \end{pmatrix} = \begin{pmatrix} \bar{1} & 0 & 0 \\ 0 & \bar{1} & 0 \\ 1 & 0 & 1 \end{pmatrix}. \quad (1)$$

Table 4
Selected geometric parameters (Å).

Br1—Ni1	2.4407 (10)	Br3—Fe3	2.3290 (16)
Ni1—N1	2.047 (5)	Br4—Fe3	2.3419 (16)
Ni1—N4	2.058 (5)	Br5—Fe3	2.2995 (16)
Ni1—N3	2.092 (5)	Br3*A*—Fe3	1.943 (10)
Ni1—N6	2.105 (5)	Br4*A*—Fe3	2.553 (15)
Br2—Fe3	2.3352 (13)	Br5*A*—Fe3	2.560 (11)
Fe1—Cent(C13—C17)	1.6358 (10)	Fe1—Cent(C18—C22)	1.6543 (10)
Fe2—Cent(C35—C39)	1.6463 (11)	Fe2—Cent(C40—C44)	1.6544 (11)

3.5. Details of the structural refinement unrelated to twinning

The Ni^{II}/Fe^{III} cation was identified and refined in a routine fashion. Selected bond distances for (1) are presented in Table 4. The refinement of the tetrahedral $[FeBr_4]^-$ anion proved to be problematic, Fig. 4. This anion is disordered over two positions related by a rotation of ∼ 62.9 (4)° about the Fe3—Br2 vector. Atoms Br3, Br4 and Br5 in the anion are disordered over two positions with the major displacement component contribution of 85.2 (2)%. In the absence of restraints and constraints, the four Fe2—Br distances to Br2 and three major component Br atoms average 2.326 (19) Å. This value is in excellent agreement with the average of 2.330 (14) Å for 216 bond distances observed in 54 $[FeBr_4]^-$ anions of trivalent Fe^{III} reported to the Cambridge Structural Database (CSD; Allen, 2002). In contrast, in six reported $[FeBr_4]^{2-}$ anions of a divalent Fe^{II} the Fe–Br distances of 2.452 (16) Å are ∼ 0.12 Å longer; thus, the assigned oxidation state of the Fe^{III} center in the anion in (1) is confirmed. In contrast, three Fe—Br bond lengths of 1.943 (10), 2.553 (15) and 2.560 (11) Å to the minor disorder component atoms Br3*a*—Br5*a* possess disparate and chemically unreasonable values. The Br—Fe—Br angles involving the minor component Br atoms deviate from 109.4° more substantially than

those to the major component Br atoms. Attempts to refine the minor component with an idealized tetrahedral geometry resulted in a configuration with abnormally large displacement ellipsoids that are considerably elongated along the Fe—Br bonds. When the restraint is relaxed, the Fe—Br distances resume their gravitation toward the freely refined values. It is possible to restrain the problematic Fe—Br distances to be chemically reasonable and identical to those in the major disorder component, however, the resultant computational refinement indicators worsen. Since no chemical or crystallographic information can be learned from the values of these Fe—Br(minor component) distances, they were refined freely. In the course of this work a refinement in which atoms Fe3 and Br2 were split in order to model the second position of the Fe3 anion in its entirety was also undertaken; anisotropic displacement parameter constraints and bond similarity restraints were used. The resultant positions of atoms Fe3/Fe3*a* and Br2/Br2*a* were very close to each other and there was still a short contact Br4*a*···C10 present, as described in the next paragraph. Thus, the model presented herein was retained.

Another nuance of the refinement is the relatively close proximity [2.35 (2) Å] of C10 and atom Br4*a* [symmetry code: $x-\frac{1}{2},\frac{1}{2}-y,z-\frac{1}{2}$], a minor component of the disordered anion. This fact implies a possible alternative position for C10, but there is no experimental indication where that second position might be, thus no attempt to refine C10 as disordered was undertaken. The close agreement of the Fe—Br distance [2.3352 (13) Å] in the $[FeBr_4]^-$ anion for the non-disordered Br2 atom with those to the three Br atoms in the major disorder component [Br3–5, range 2.2995 (16)–2.3419 (16) Å] signifies that the major disordered component of 85.5 (2)% defines the anion's geometry reasonably well, such that the minor disordered component can be neglected.

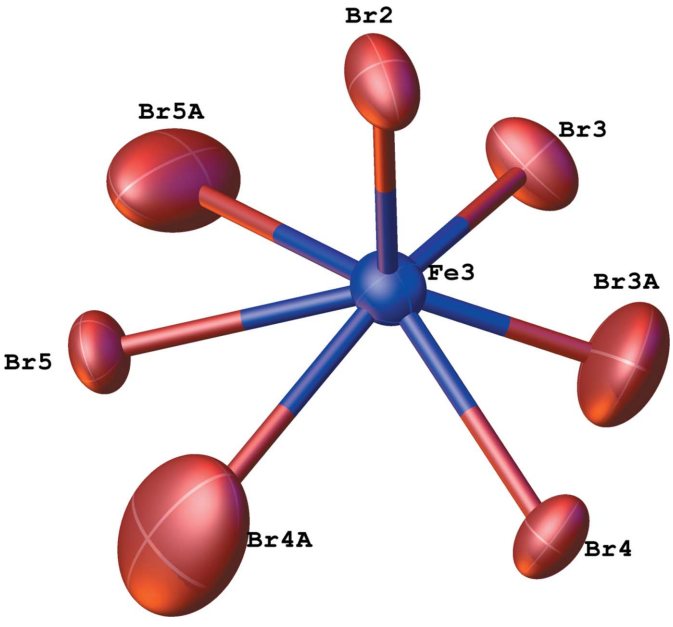

Figure 4
A drawing of the tetrahedral $[FeBr_4]^-$ anion shown with all observed positions of the Br atoms. Atoms Br3–5 are disordered over two positions; the major component with atoms Br3, Br4 and Br5 has a site occupancy of 85.5 (2)%, whereas the minor component atoms Br3*a*–5*a* are present 14.5 (2)% of the time.

4. Discussion of the crystal structure of (1)

(Pyrazol-1-ylmethyl)pyridine compounds have been used as ligands in the preparation of metal complexes since they were first prepared by Steel and co-workers in 1986 (House *et al.*, 1986). In their use as ligands, (pyrazol-1-ylmethyl)pyridine compounds usually behave as bidentate ligands, binding to metals through a pyrazolyl nitrogen and the pyridinyl N atoms (Ojwach *et al.*, 2007, 2009). Recently a modification of (pyrazol-1ylmethyl)pyridine *via* addition of the methylene bridge to give (pyrazol-1-ylpropan-2-ol)pyridine showed a different coordination chemistry. Reactions of these (pyrazol-1-ylpropan-2-ol)pyridine compounds with $NiCl_2$, $CuCl_2$ and $ZnCl_2$ invariably led to chloride eliminations from the metal coordination sphere (Gennari *et al.*, 2007). Noteworthy is that the reaction stoichiometry played a prominent role in determining the reaction product. When the reaction ratio was 2:1, (pyrazol-1-ylpropan-2-ol)pyridine (**L1**OH) reacted with $NiCl_2$ or $CoCl_2$ to form $[M(\mathbf{L1}OH)_2]Cl_2$ (M = Ni, Cu), whereas a 1:1 reaction ratio of each MCl_2 compound produced $[M(\mathbf{L1}OH)_2][MCl_4]$ (M = Ni, Cu, Zn; Gennari *et al.*, 2007). We have recently investigated the reaction of (3-ferrocenyl-5-ethylcarboxylate-pyrazol-1-ylmethyl)pyridine (**L2**) with nickel dibromide and found that it reacted with $NiCl_2$ to form the complex salt $[Ni(\mathbf{L2})_2Br][FeBr_4]$ (1), whose different stoichiometry illustrates another type of product for a derivative of (pyrazol-1-ylmethyl)pyridine.

Both the cation and anion of (1) possess approximate C_2 symmetry, a fact partly responsible for the observed twinning. The r.m.s. deviation of the non-C atoms superimposed on their counterparts when the monocation is rotated by 180° about the Ni1–Br1 vector is 0.24 Å (Macrae *et al.*, 2008). The localized ligand coordination of the Ni^{II} center is distorted trigonal bipyramidal: atoms Br1 and the pyridinyl N1 and N4 atoms form the basal trigonal plane, with the pyrazolato N3 and N6 atoms residing above and below the plane such that the N3—Ni1—N6 angle spans 178.2 (2)°. The Ni1—Br1 distance of 2.4407 (10) Å is in excellent agreement with the average Ni(five-coordinate)—Br(terminal) distance of 2.42 (5) Å obtained by averaging 135 values in 84 relevant structures reported in the CSD. This and other cited CSD searches were conducted with tight-search criteria (namely, three-dimensional coordinates determined, R factor < 0.05, no errors, not polymeric, no powder structures). For comparison, the Ni(four-coordinate)—Br(terminal) and Ni(six-coordinate)—Br(terminal) distances averaged to be 2.35 (3) and 2.56 (8) Å, consistent with the expected trend of bond elongation concomitant with an increasing coordination number. Both bidentate ligands form six-membered heterocycles in a boat conformation. Both ferrocenyl units exhibit normal, essentially eclipsed geometries.

5. Conclusions

We have provided a detailed account of the structural investigation of a pseudo-merohedrally twinned organometallic crystal. The non-crystallographic symmetry of the crystal in question (twofold pseudo-symmetry) complicated the detection of the correct space group. An explanation of the steps undertaken to elucidate and to account for the observed twinning is provided for assistance in the studies of similar non-routine structural problems with the currently available programs such as *CELL_NOW*, *OLEX*2, *PLATON*, *SHELXL* and *XPREP*.

The authors are grateful to Dr Victor G. Young (University of Minnesota) and Professor George M. Sheldrick (University of Göttingen) for informative discussions of twin handling, and Professor Larry Dahl (University of Wisconsin-Madison) for constructive comments. We thank the NRF-DST Centre of Excellence in Catalysis (*c** change) and the University of Johannesburg for funding.

References

Allen, F. H. (2002). *Acta Cryst.* B**58**, 380–388.
Bruker AXS Inc. (2007). *APEX*2. Bruker AXS Inc., Madison, WI, USA.
Bruker AXS Inc. (2011*a*). *SADABS*. Bruker AXS Inc., Madison, WI, USA.
Bruker AXS Inc. (2011*b*). *SAINT*. Bruker AXS Inc., Madison, WI, USA.
Dolomanov, O. V., Bourhis, L. J., Gildea, R. J., Howard, J. A. K. & Puschmann, H. (2009). *J. Appl. Cryst.* **42**, 339–341.
Donnay, G. & Donnay, J. D. H. (1974). *Can. Mineral.* **12**, 422–425.
Flack, H. D. (1983). *Acta Cryst.* A**39**, 876–881.
Gennari, M., Tegoni, M., Lanfranchi, M., Pellinghelli, M. A. & Marchio, L. (2007). *Inorg. Chem.* **46**, 3367–3377.
Guevarra, J., van Smaalen, S., Rotiroti, N., Paulmann, C. & Lichtenberg, F. (2005). *J. Solid State Chem.* **178**, 2934–2941.
Guzei, I. A., Spencer, L. C., Munyaneza, A. & Darkwa, J. (2012). *Acta Cryst.* E**68**, 35–36.
Guzei, I. A., Wang, C., Zhan, Y., Dolomanov, O. V. & Cheng, Y.-Q. (2009). *Acta Cryst.* C**65**, o521–o524.
Herbst-Irmer, R. (2006). *Crystal Structure Refinement – A Crystallographer's Guide to SHELXL*, Ch. 7., edited by P. Mueller. Oxford University Press.
Herbst-Irmer, R. & Sheldrick, G. M. (1998). *Acta Cryst.* B**54**, 443–449.
Herbst-Irmer, R. & Sheldrick, G. M. (2002). *Acta Cryst.* B**58**, 477–481.
House, D. A., Steel, P. J. & Watson, A. A. (1986). *Aust. J. Chem.* **39**, 1525–1536.
Lebedev, A. A., Vagin, A. A. & Murshudov, G. N. (2006). *Acta Cryst.* D**62**, 83–95.
Macrae, C. F., Bruno, I. J., Chisholm, J. A., Edgington, P. R., McCabe, P., Pidcock, E., Rodriguez-Monge, L., Taylor, R., van de Streek, J. & Wood, P. A. (2008). *J. Appl. Cryst.* **41**, 466–470.
Noe, E. A., Pawar, D. M. & Fronczek, F. R. (2008). *Acta Cryst.* C**64**, o67–o68.
Ojwach, S. O., Guzei, I. A., Benade, L. L., Mapolie, S. F. & Darkwa, J. (2009). *Organometallics*, **28**, 2127–2133.
Ojwach, S. O., Guzei, I. A., Darkwa, J. & Mapolie, S. F. (2007). *Polyhedron*, **26**, 851–861.
Parsons, S. (2003). *Acta Cryst.* D**59**, 1995–2003.
Sheldrick, G. M. (2006). *XPREP*. University of Goettingen. p. *XPREP*.
Sheldrick, G. M. (2008*a*). *Acta Cryst.* A**64**, 112–122.
Sheldrick, G. M. (2008*b*). *CELL_NOW*. University of Göttingen, Germany.
Spek, A. L. (2009). *Acta Cryst.* D**65**, 148–155.
Wilson, A. J. C. (1995). Editor. *International Table for Crystallography*, Vol. C, p. 883. Dordrecht: Kluwer Academic Publishers.
Zwart, P. H., Grosse-Kunstleve, R. W., Lebedev, A. A., Murshudov, G. N. & Adams, P. D. (2008). *Acta Cryst.* D**64**, 99–107.